Generic Rugged Landscapes under Strain and the Possibility of Rejuvenation in Glasses

Brittany A. Isner and Daniel J. Lacks

Department of Chemical Engineering, Case Western Reserve University, Cleveland, Ohio 44106, USA

(Received 26 August 2005; published 20 January 2006)

A strain-dependent random landscape model shows that many aspects of the mechanical response of disordered materials are universal, and arise from the rugged nature of the energy landscape. Simulations with this model demonstrate that states produced by mechanical deformation will generally be distinct from the states traversed during thermal aging. This behavior is a generic consequence of a rugged energy landscape, and is independent of any specific microstructure of the material. Thus, mechanical deformation does not literally "rejuvenate" a material, although the states produced by mechanical deformation may in some ways resemble less aged systems.

DOI: 10.1103/PhysRevLett.96.025506 PACS numbers: 61.43.Fs, 62.20.Fe

The relationship between the aging process and mechanical deformation in glassy materials is not fully understood. While aging alters mechanical properties, mechanical deformation also alters the aging process. A number of experiments suggest that mechanical deformation reverses aging, or "rejuvenates" the material—this effect has been suggested in regard to polymer materials [1], colloidal glasses, and pastes [2–7], and even biological cytoskeletons [8]. However, experiments by McKenna and others suggest that mechanical deformation does not really rejuvenate the material [9]. For example, in some cases mechanical deformation does not alter the state of the material even when evidence (based on relaxation times) suggests rejuvenation [10,11], and in other cases mechanical deformation appears to move the material to states that are distinct from any state that occurs during the aging process [9,12,13]. Also, some experiments suggest that mechanical deformation can accelerate, rather than reverse, the aging process [3,14].

The properties of disordered materials, including glasses, colloids, foams, granular materials, etc. are universal in many ways [15,16]. The universality has been attributed to the existence of many local optima for particle packing. These effects are captured by the energy landscape framework, in which the state of the system is characterized by the ensemble of energy minima visited by the system [17,18]. The landscape framework has also been used to study nonphysical phenomena ranging from biological evolution [19] to business management [20], using random landscape models such as the N-K model [19] to represent generic rugged landscapes.

In the present investigation, aging and mechanical deformation are examined for a random landscape model. While molecular simulations have been used to study these phenomena in atomistic systems [21–23], the use of a random landscape model allows the determination of generic effects that arise solely on the basis of a rugged energy landscape, rather than on the specific microstructure of a material.

The strain-dependent modification of the N-K model introduced by Wilke and Martinetz [24] is used. The model consists of N components that exist in one of two "positions"; the position of component i is denoted by m_i. The energy is a function of the positions of each of the components, $E = E(m_1, m_2, \ldots, m_N)$, and is obtained as

$$E = -\frac{1}{N}\sum_{i=1}^{N}\frac{1}{2}\{1 + \sin[2\pi(a_i + \gamma b_i)]\}, \tag{1}$$

where γ is the "strain" and a_i and b_i are parameters that determine the contribution of component i to the energy. Each component interacts with K other components, so that a_i and b_i depend on the position of component i (m_i), and additionally on the position of K other components (denoted by $m_1^i, m_2^i, \ldots, m_K^i$). The parameters $a_i(m_i, m_1^i, m_2^i, \ldots, m_K^i)$ are assigned random values between 0 and 1 for each combination of $m_i, m_1^i, m_2^i, \ldots, m_K^i$, and the parameters $b_i(m_i, m_1^i, m_2^i, \ldots, m_K^i)$ are assigned random values between -1 and 1 for each combination of $m_i, m_1^i, m_2^i, \ldots, m_K^i$. The energy landscape is smooth with one energy minimum for $K = 0$, and rugged and fully uncorrelated for $K = N - 1$; results are shown here for $N = 48$ and $K = 16$, but similar results are obtained with other values of K and N (for $K > 0$). The stress σ and elastic modulus B are evaluated analytically as the first and second derivatives, respectively, of Eq. (1) with respect to strain.

First, Monte Carlo (MC) simulations are carried out to determine the regions of the energy landscape visited by the system at equilibrium. The MC simulations begin at a randomly chosen configuration, and are run for N_{MC} steps. In each MC step, the position of a randomly selected component is changed, which changes the energy by ΔE; this step is accepted if $r < \exp(-\Delta E/T)$, where r is a random number between 0 and 1. Energy minima visited by the system are found by steepest descent energy minimizations that begin from configurations during the MC trajectory (at each step in the minimization procedure the position is changed for the component that gives the largest decrease in energy, and these steps repeated until no further position changes decrease the energy); the energy and elastic modulus at an energy minimum are designated E_s

and B_s, respectively. The simulations are repeated for many landscapes (i.e., different values of a_i and b_i), to obtain the ensemble averages $\langle E_s \rangle$ and $\langle B_s \rangle$. Equilibrium results correspond to results in the $N_{\mathrm{MC}} \to \infty$ limit.

Equilibrium results for $\langle E_s \rangle$ as a function of temperature, shown in Fig. 1, are qualitatively identical to the results of molecular simulations of atomistic systems [25]. The system visits lower energy states as the temperature decreases, and equilibrated results cannot be obtained below a glass transition temperature (~0.45) because equilibration occurs on time scales longer than the time scales of the simulations.

Following a change in temperature, the values of $\langle E_s \rangle$ and $\langle B_s \rangle$ change with time ("thermal aging") until equilibrium is reached. Figure 2 shows the values of $\langle E_s \rangle$ and $\langle B_s \rangle$ during thermal aging, along with the values for the equilibrated systems. The same line in the $\langle E_s \rangle$ and $\langle B_s \rangle$ plane describes the states visited during thermal aging and the equilibrium states at different temperatures; this behavior is observed in molecular simulations for slow cooling rates [26–28], while very fast cooling moves the system to states that are distinct from equilibrium states [27,28]. Note that this method of monitoring aging differs from the often-used method of monitoring correlation functions.

Glasses are obtained from equilibrated liquids by infinitely fast cooling to zero temperature, so that the fictive temperature (T_f) of the glass is simply the temperature of the equilibrium liquid before cooling. The fictive temperature has been used to quantify the extent of aging in glasses, with more highly aged glasses having a lower T_f [29].

The mechanical deformation of the glasses is examined at zero temperature, in order to separate the effects of mechanical deformation on the state of the glass from the effects of thermal fluctuations. Strain is imposed in the zero temperature and zero strain-rate limits by incrementing the strain (γ) in very small steps and minimizing the energy after each step (the system always remains at an energy minimum in these limits). Strain increments of 0.003–0.006 are used, which approximate continuous change.

The stress-strain curves, shown in Figs. 3(a)–3(c) look like typical stress-strain curves of real glassy materials: an elastic regime occurs at low strains, yielding occurs at intermediate strains, a plastic flow regime occurs at high strains, and hysteresis occurs as the strain is reversed. A comparison of results for different fictive temperatures shows that aging alters the mechanical response by increasing the elastic modulus and yield stress, and creating a pronounced stress overshoot. The same effects of aging on the mechanical response have been observed experimentally in polymer materials [30–33], colloidal pastes and glasses [4,5], and molecular simulations of simple glasses [21,34,35].

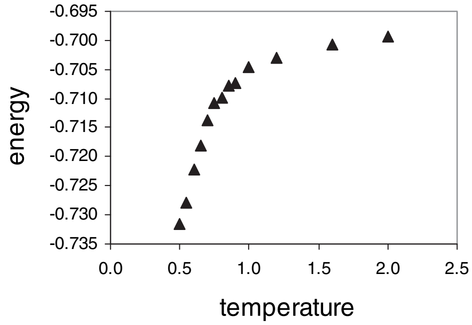

FIG. 1. Equilibrium results for the average energy of energy minima visited by system.

The results for $\langle E_s \rangle$ as a function of strain γ are shown in Figs. 3(d)–3(f). Changes in energy with strain can occur in two ways: by the explicit strain dependence of the energy [Eq. (1)], or by a change in the positions of the components (i.e., $m_1, m_2, \ldots, m_N$). In these zero temperature limit simulations, the components can change positions only after strain destroys an energy minimum; the strain-induced destruction of energy minima, which has been demonstrated previously in a strain-dependent *N-K* model [36], also occurs in atomistic systems [37]. Changes in energy associated with the explicit strain dependence are given by $dE = \sigma d\gamma$ and are fully reversible, while changes in energy due to position changes are characterized by $dE < 0$. Upon increasing strain, $\langle E_s \rangle$ initially decreases slightly due to position changes (since σ is initially small), before $\langle E_s \rangle$ increases due the explicit strain dependence of the energy as σ becomes larger. In the plastic flow state, the two mechanisms of energy change balance to yield a constant $\langle E_s \rangle$. Upon decreasing γ, $\langle E_s \rangle$ initially decreases significantly because *both* mechanisms act to decrease the energy. As shown in Fig. 3(d), small strain cycles move the system to deeper energy minima (i.e., in the same direction as aging). In contrast, as shown in Fig. 3(f), large strain cycles move the system to shallower energy minima (i.e., in the opposite direction as aging). Intermediate strain cycles move more highly aged

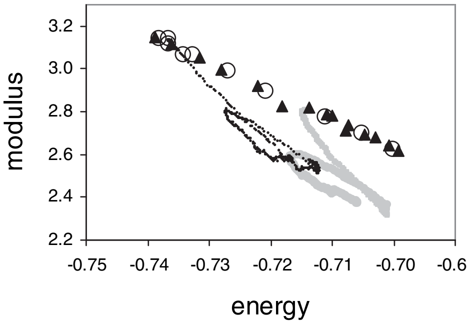

FIG. 2. Average elastic modulus and energy at energy minima. Triangles: equilibrium results. Circles: results during the aging process that follows a temperature decrease. Gray line: results during strain cycle for glass with $T_f = 0.7$. Black dots: finite temperature results during strain cycle for glass at $T = 0.2$, with strain rate of 100 MC steps per strain increment of 0.003. Strain cycle results are for a strain amplitude of 0.6.

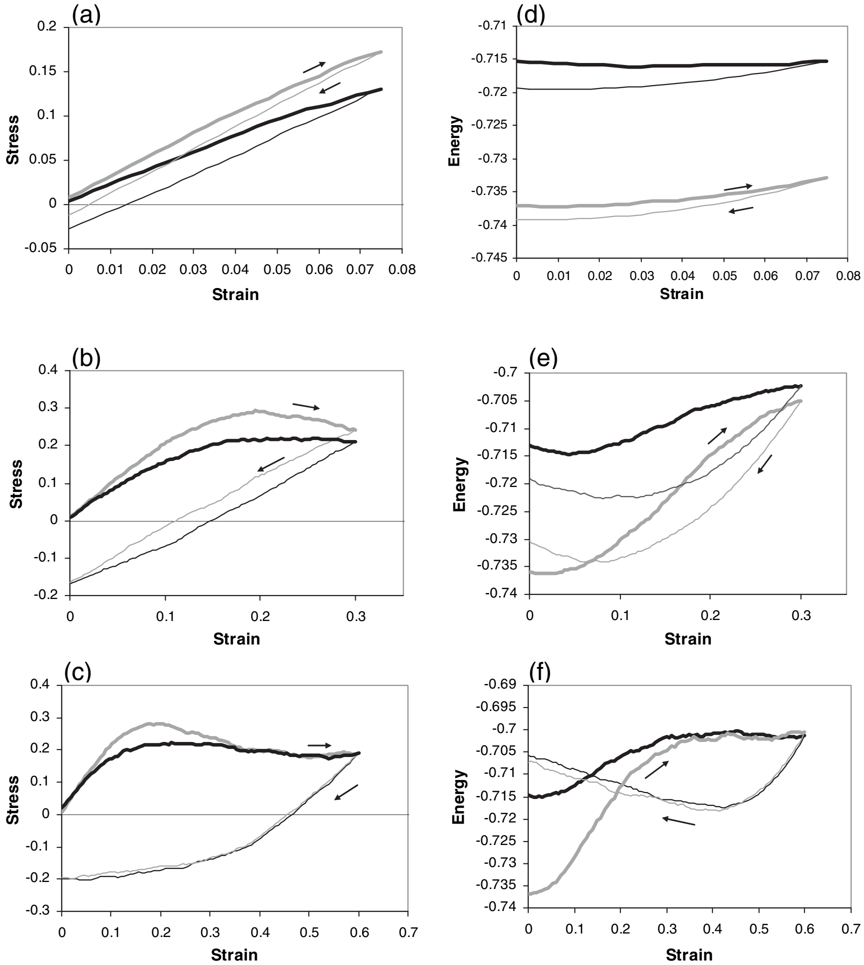

FIG. 3. (a)–(c) Average stress and (d)–(f) average energy during deformation in the zero-temperature and zero-strain-rate limits. Black lines are for $T_f = 0.7$, and gray lines are for $T_f = 0.5$. Thick lines are for increasing strain, and thin lines are for decreasing strain.

systems to shallower energy minima, and less aged systems to deeper energy minima [Fig. 3(d)]. Identical effects have been observed in molecular simulations of simple atomistic systems [22].

The values of $\langle E_s \rangle$ and $\langle B_s \rangle$ for these strained systems are shown in Fig. 2, where they are compared to results for equilibrated systems and for systems undergoing thermal aging. The states produced by mechanical deformation are characterized by different combinations of $\langle E_s \rangle$ and $\langle B_s \rangle$, which shows that these states are distinct from equilibrium states and states traversed by the system during thermal aging. In other words, large strains do not literally rejuvenate the system, but the states produced by large strains may resemble the higher temperature states in some ways (e.g., depths of energy minima, characteristic relaxation times). Thus, the extent of aging cannot be fully described by only one variable, whether this one variable is a fictive temperature or a relaxation time.

Results at finite temperature and strain rate were also obtained by carrying out MC simulations after each strain increment. These results, shown in Fig. 2, demonstrate that the picture that emerges from the results in the zero-temperature and zero-strain-rate limits is also appropriate at finite temperatures and strain rates.

To understand why large mechanical deformation produces states that are distinct from high temperature states, the behavior in an N-K model with $N = 4$ and $K = 3$ is analyzed—the small dimensionality of this $N = 4$ model allows the complete characterization of the system. Figure 4 shows all energy minima (gray lines) for this model with one set of model parameters (a_i and b_i). The depths of energy minima change as the system is strained. The number of energy minima also change with strain, due to their creation and destruction [36,37]; there are 3 energy minima at zero strain, but the number of energy minima varies between 2 and 6 for strains between 0 and 1. The black lines in Fig. 4 show how the state of the system changes as strain is increased in the zero-temperature and zero-strain-rate limits: the system remains in an energy minimum until this minimum is destroyed, at which point it relaxes to a different energy minimum by the steepest descent path. As a result of these athermal dynamics, all 3 initial states move to the identical state for $\gamma > 0.71$ (and thus will be in identical states thereafter, even if the strain is reversed). In contrast, the dynamics due to thermal fluctuations would cause *all* energy minima to be visited at high temperature. Thus, the athermal dynamics due to mechanical deformation, and the thermal dynamics at high

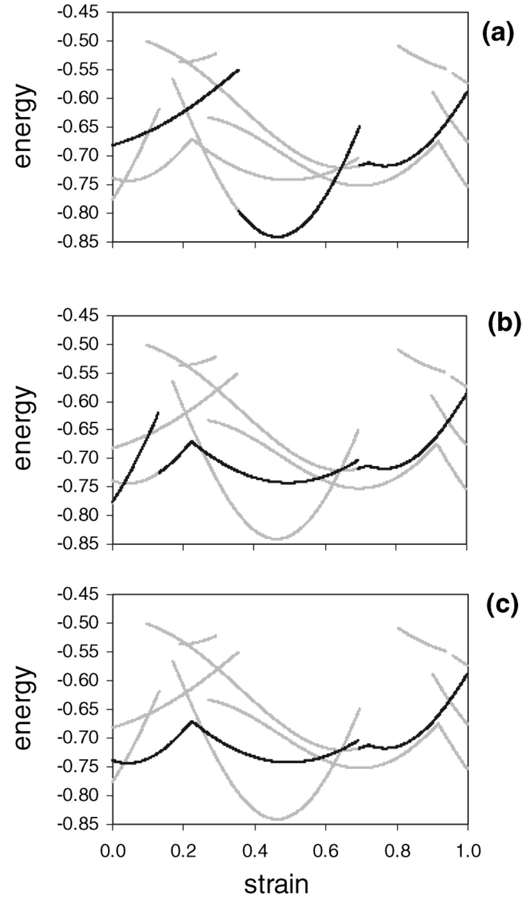

FIG. 4. Changes in the state of an $N = 4$ system as the system is strained. These results are for a single system (not ensemble averages). Gray lines show the energies of all energy minima. Black lines show the state of the system, when the system initially occupies (at zero strain) the (a) high energy state, (b) low energy state, and (c) middle energy state.

temperature, produce different occupancies of energy minima and thus different states of the system.

In summary, the present investigation shows that mechanical deformation does not really rejuvenate a material, because it does not bring the material to states that characterize earlier stages in the aging process. This behavior is a consequence of the ruggedness of the landscape (i.e., the existence of many local energy minima), rather than any particular microstructure of the material, and thus is expected to be relevant to all types of disordered materials.

This material is based upon work supported by the National Science Foundation under Grant No. DMR-0402867.

[1] L. C. E. Struik, *Physical Aging in Amorphous Polymers and Other Materials*, (Elsevier, New York, 1978).
[2] M. Cloitre, R. Borrega, and L. Leibler, Phys. Rev. Lett. **85**, 4819 (2000).
[3] V. Viasnoff and F. Lequeux, Phys. Rev. Lett. **89**, 065701 (2002).
[4] D. Bonn *et al.*, Phys. Rev. Lett. **89**, 015701 (2002).
[5] C. Derec *et al.*, Phys. Rev. E **67**, 061403 (2003).
[6] F. Ozon *et al.*, Phys. Rev. E **68**, 032401 (2003).
[7] S. Kaloun *et al.*, Phys. Rev. E **72**, 011401 (2005).
[8] P. Busac *et al.*, Nat. Mater. **4**, 557 (2005).
[9] G. B. McKenna, J. Phys. Condens. Matter **15**, S737 (2003).
[10] A. Lee and G. B. McKenna, Polymer, **31**, 423 (1990).
[11] M. M. Santore, R. S. Duran, and G. B. McKenna, Polymer **32**, 2377 (1991).
[12] H. G. H. van Melick *et al.*, Polymer **44**, 1171 (2003).
[13] D. Cangialosi *et al.*, J. Chem. Phys. **122**, 064702 (2005).
[14] D. M. Colucci, P. A. O'Connell, and G. B. McKenna, Polym. Eng. Sci. **37**, 1469, (1997).
[15] P. Sollich *et al.*, Phys. Rev. Lett. **78**, 2020 (1997).
[16] A. J. Liu and S. R. Nagel, Nature (London) **396**, 21 (1998).
[17] F. H. Stillinger and T. A. Weber, Science **225**, 983 (1984).
[18] P. G. Debenedetti and F. H. Stillinger, Nature (London) **410**, 259 (2001).
[19] S. A. Kauffman, *The Origins of Order* (Oxford University Press, Oxford, 1993).
[20] N. Siggelkow and J. W. Rivkin, Organization Science: A Journal of the Institute of Management Sciences **16**, 101 (2005).
[21] M. Utz *et al.*, Phys. Rev. Lett. **84**, 1471 (2000).
[22] D. J. Lacks and M. J. Osborne, Phys. Rev. Lett. **93**, 255501 (2004).
[23] M. L. Wallace and B. Joos, cond-mat/0506737.
[24] C. O. Wilke and T. Martinetz, Phys. Rev. E **60**, 2154 (1999).
[25] S. Sastry, P. G. Debenedetti, and F. H. Stillinger, Nature (London) **393**, 554 (1998).
[26] W. Kob, F. Sciortino, and P. Tartaglia, Europhys. Lett. **49**, 590 (2000).
[27] N. Giovambattista, H. E. Stanley, and F. Sciortino, Phys. Rev. E **69**, 050201(R) (2004).
[28] I. Saika-Voivod and F. Sciortino, Phys. Rev. E **70**, 041202 (2004).
[29] A. Q. Tool, J. Am. Ceram. Soc. **29**, 240 (1946).
[30] J. H. Golden, B. L. Hmammant, and E. A. Hazell, J. Appl. Polym. Sci. **11**, 1571 (1967).
[31] J. M. Hutchinson, S. Smith, B. Horne, and G. M. Gourlay, Macromolecules **32**, 5046 (1999).
[32] H. G. H. van Melick, L. E. Govaert, and H. E. H. Meijer, Polymer **44**, 3579 (2003).
[33] L. Guadagno *et al.*, J. Polym. Sci., Part B: Polym. Phys. **37**, 173 (1999).
[34] F. Varnik, L. Bocquet, and J.-L. Barrat, J. Chem. Phys. **120**, 2788 (2004).
[35] M. J. Osborne and D. J. Lacks, J. Phys. Chem. B **108**, 19 619 (2004).
[36] D. L. Nikolic and D. J. Lacks, J. Theor. Biol. **221**, 259 (2003).
[37] D. L. Malandro and D. J. Lacks, Phys. Rev. Lett. **81**, 5576 (1998).